Vol. 40 — N° 2 06 16 P. 157–172

GEOSTANDARDS and GEOANALYTICAL RESEARCH

Secondary Ion Mass Spectrometry Bias on Isotope Ratios in Dolomite–Ankerite, Part I: $\delta^{18}O$ Matrix Effects

Maciej G. **Śliwiński** (1, 2)*, Kouki **Kitajima** (1, 2, 3), Reinhard **Kozdon** (1, 4), Michael J. **Spicuzza** (1, 2), John H. **Fournelle** (2), Adam **Denny** (1, 2) and John W. **Valley** (1, 2, 3)

(1) WiscSIMS, Department of Geoscience, University of Wisconsin-Madison, Madison, WI, 53706, USA
(2) Department of Geoscience, University of Wisconsin-Madison, Madison, WI, 53706, USA
(3) Department of Geoscience, NASA Astrobiology Institute, University of Wisconsin-Madison, Madison, WI, 53706, USA
(4) Department of Marine and Coastal Sciences, Rutgers, The State University of New Jersey, New Brunswick, NJ, 08901-8521, USA
* Corresponding author. e-mail: msliwinski@wisc.edu

We document the development of a suite of carbonate mineral reference materials for calibrating SIMS determinations of $\delta^{18}O$ in samples with compositions along the dolomite–ankerite solid solution series [$CaMg(CO_3)_2$–$CaFe(CO_3)_2$]. Under routine operating conditions for the analysis of carbonates for $\delta^{18}O$ with a CAMECA IMS 1280 instrument (at WiscSIMS, University of Wisconsin-Madison), the magnitude of instrumental bias along the dolomite–ankerite series decreased exponentially by ~ 10‰ with increasing Fe content in the dolomite structure, but appeared insensitive to minor Mn substitution [< 2.6 mol% Mn/(Ca+Mg+Fe+Mn)]. The compositional dependence of bias (i.e., the sample matrix effect) was calibrated using the Hill equation, which relates bias to the Fe# of dolomite–ankerite [i.e., molar Fe/(Mg+Fe)] for thirteen reference materials (Fe# = 0.004–0.789); for calibrations employing either 10 or 3 μm diameter spot size measurements, this yielded residual values ≤ 0.3–0.4‰ relative to CRM NBS 19 for most reference materials in the suite. Analytical precision was ± 0.3‰ (2*s*, standard deviations) for 10-μm spots and ± 0.7‰ (2*s*) for 3-μm spots, based on the spot-to-spot repeatability of a drift monitor material that 'bracketed' each set of ten sample-spot analyses. Analytical uncertainty for individual sample analyses was approximated by a combination of precision and calibration residual values (propagated in quadrature), suggesting an uncertainty of ± 0.5‰ (2*s*) for 10-μm spots and ± 1‰ (2*s*) for 3-μm spots.

Keywords: secondary ion mass spectrometry, oxygen isotopes, dolomite, ankerite, matrix effects.

Received 20 Feb 15 – Accepted 13 Jun 15

Nous documentons le développement d'une série de minéraux carbonatés de référence pour calibrer les déterminations à la SIMS du $\delta^{18}O$ dans les échantillons avec des compositions se situant le long de la solution solide dolomite-ankérite [$CaMg(CO_3)_2$–$CaFe(CO_3)_2$]. Dans des conditions de fonctionnement en routine pour l'analyse du $\delta^{18}O$ des carbonates avec un instrument IMS 1280 (WiscSIMS, Université du Wisconsin, Madison), l'ampleur du biais instrumental le long de la série dolomite-ankérite diminue de façon exponentielle de ~ 10‰ avec l'augmentation de la teneur en Fe dans la structure de la dolomite, mais semble insensible à la substitution mineure Mn (< 2,6 mol% Mn/(Ca + Mg + Fe + Mn)). La dépendance du biais à la composition (i.e., l'effet de la matrice de l'échantillon) a été calibrée en utilisant l'équation de Hill, qui relie le biais au Fe# de la solution solide dolomite-ankérite (i.e., Fe/(Mg + Fe) molaire) pour treize matériaux de référence (Fe# = 0,004–0,789); pour les calibrations employant des diamètres de spots de 10 μm ou de 3 μm, cela a donné des valeurs résiduelles ≤ 0,3–0,4‰ par rapport au CRM NBS 19 pour la plupart des matériaux de référence de la suite. La précision analytique était de ± 0,3‰ (2s) pour les spots de 10 μm et de ± 0,7‰ (2s) pour les spots de 3 μm, basé sur la répétabilité spot à spot d'un matériau de contrôle de la dérive encadrant chaque ensemble de dix analyses ponctuelles d'échantillon. L'incertitude analytique pour les analyses d'un échantillon individuel a été approchée par une combinaison des valeurs de précision et d'étalonnage résiduelles (propagée en quadrature), ce qui suggère une incertitude de ± 0,5‰ (2s) pour les spots de 10 μm et de ± 1‰ (2s) pour les spots de 3 μm.

Mots-clés : SIMS, isotopes de l'oxygène, dolomite, ankérite, effets de matrice.

doi: 10.1111/j.1751-908X.2015.00364.x

The fractionation of stable carbon and oxygen isotopes ($\delta^{13}C$ and $\delta^{18}O$) in carbonate minerals yields widely employed and well-established proxies in the geosciences that are often used to constrain conditions during sediment diagenesis (e.g., Arthur *et al.* 1983, Dutton and Land 1985, Longstaffe 1989, Fayek *et al.* 2001) and metamorphism (e.g., Baumgartner and Valley 2001, Bowman *et al.* 2009, Ferry *et al.* 2014), or to reconstruct secular changes of climatic and palaeoceanographic conditions on Earth (e.g., Veizer *et al.* 1997, Jaffrés *et al.* 2007, Prokoph *et al.* 2008, Orland *et al.* 2009, Kozdon *et al.* 2011) and the evolution of the early Martian environment (e.g., Valley *et al.* 1997, Leshin *et al.* 1998, Eiler *et al.* 2002, Holland *et al.* 2005, Shaheen *et al.* 2015). The application of secondary ion mass spectrometry (SIMS) in the Earth and space sciences offers an unprecedented spatial resolution for precisely investigating isotopic records at the micrometre scale. The ability to make these measurements *in situ* from a grain mount or thin section allows measurement of zoning and correlation to textures. However, a critical aspect of further advancing analytical methods of carbonate mineral analysis is the continued development of reference materials to correct for complex but systematic instrumental mass fractionation (IMF) effects (hereafter referred to as 'bias') that can significantly affect analytical accuracy.

An isotope ratio measured by SIMS can be highly precise. For example, a spot-to-spot precision of $\leq 0.3‰$ (2*s*, standard deviation) is routinely achievable in measurements of $\delta^{18}O$ in many silicate and carbonate minerals (Valley and Kita 2009). However, measured isotope ratios are inherently different from the true isotopic composition of an element within a sample material (Hervig *et al.* 1992, Eiler *et al.* 1997; Valley and Kita 2009). This is due in part to mass fractionation that occurs: (1) during the production and acceleration of ions from the sample (Fitzsimons *et al.* 2000, Huberty *et al.* 2010, Kita *et al.* 2011), (2) during secondary ion transmission through the mass spectrometer and (3) during detection. Mass fractionation associated with the interaction between the primary ion beam and the sample is in turn related to the chemical composition and atomic structure of the sample. Collectively, these instrumental mass fractionation effects can be referred to as the measurement or instrumental 'bias', *sensu* VIM (2008). The term 'bias' denotes an 'estimate of a systematic measurement error', the causes of which can be known or unknown (2.18, VIM 2008). A systematic measurement error is the 'component of measurement error that in replicate measurements remains constant or varies in a predictable manner' (2.17, VIM 2008). Importantly, 'a correction can be applied to compensate for a known systematic measurement error' (2.17 NOTE 2, VIM 2008). There is at present no adequate theoretical model for accurately predicting secondary ion yields or isotope ratios during the sputtering process; accurate isotope ratio measurements thus require the use of matrix-matched reference materials (RMs) that are analysed together with unknown samples under consistent, analytical session-specific conditions and configurations of the ion microprobe (Hervig *et al.* 1992, Eiler *et al.* 1997, Fitzsimons *et al.* 2000, Valley and Kita 2009, Ickert and Stern 2013). For minerals exhibiting solid solution behaviour, accurate isotope ratio determinations are possible only if a sufficient number of RMs is employed to empirically characterise, on a session-by-session basis, how instrumental bias varies as a function of chemical composition.

Instrumental bias effects for $\delta^{18}O$ analysis of carbonates by SIMS have been studied for various end-member compositions (e.g., Eiler *et al.* 1997, 2002, Valley *et al.* 1997, Kozdon *et al.* 2009, Valley and Kita 2009, Rollion-Bard and Marin-Carbonne 2011), but the functional relations between bias and cation substitution along the various solid solutions are poorly known. The focus of this study is a thorough empirical characterisation of SIMS $\delta^{18}O$ bias for the dolomite–ankerite series ($CaMg(CO_3)_2$–$CaFe(CO_3)_2$), which has previously been investigated only to a limited extent (e.g., Riciputi *et al.* 1998, Fayek *et al.* 2001). We report here on the development of a suite of $\delta^{18}O$ reference materials and a bias calibration, while the nature of $\delta^{13}C$ bias for the dolomite–ankerite series is the focus of part II of this study.

The motivation for this two-part study stems from the importance of carbonate $\delta^{18}O$ and $\delta^{13}C$ records in the geosciences, especially in the field of reconstructing past climatic conditions throughout the evolution of the Earth system, in addition to their prevalent use in the field of sediment diagenesis. Sediments and sedimentary rocks of pre-Holocene age form a carapace that covers approximately 66% of the Earth's surface (Blatt and Jones 1975) and record the evolution of marine and terrestrial environments over the course of the last ~ 3.8 billion years. Carbonate rocks composed largely of the minerals calcite/aragonite and those of the dolomite–ankerite series comprise some 15% of this record (Tucker and Wright 1990); their occurrence is widespread through time, dating back to the Archaean (e.g., Veizer *et al.* 1989, Veizer *et al.* 1990). Further, carbonate minerals feature prominently in the fossil record, as carbonate precipitation is strongly mediated by biological and biochemical processes (e.g., Tucker and Wright 1990). Fossils contained within sedimentary sequences record the first appearance and subsequent evolution of life; they occur in the form of physical bodily remains (e.g., mineralised exoskeletons and other 'hard

parts'), microbially induced sedimentary structures (e.g., stromatolites) or in the form of chemical fingerprints of biological activity (e.g., carbon isotope fractionation signatures). The earliest, readily observable evidence of the latter remains preserved as carbonate-cemented stromatolitic structures that date back to 3.47 Ga (e.g., from North Pole Dome, Pilbara Craton, Australia; Buick 2003). These are layered mounds of sediment accreted through the growth of microbial mats and cemented by precipitates formed by metabolically induced changes in the local chemistry of the surrounding microenvironment. Chemical evidence of life, in the form of a biologically induced fractionation of carbon isotopes preserved in kerogen (fossil organic matter) and its hosting carbonate sediment, dates back somewhat further to 3.52 Ga (Coonterunah Group of NW Australia; Buick 2003).

From the perspective of economic geology, interest in isotopic studies of carbonates – as a means of understanding their genesis and alteration history – derives from the fact that carbonates are of considerable importance as hydrocarbon reservoirs and as hosts for ore deposits (e.g., dolomite-hosted Mississippi Valley type Pb and Zn ores; see review by Warren 2000). Approximately 50% of the world's major petroleum reserves are contained within carbonate rocks (Tucker 2001, Ahlbrandt *et al.* 2005), about half of which are dolomites (Zenger *et al.* 1980, Warren 2000). Carbonate cements, comprised largely of calcite, dolomite–ankerite and siderite, are among the predominant authigenic precipitates in sandstones; understanding their evolution and spatial distribution in relation to progressive sediment burial and diagenesis is thus of importance to reservoir evaluation (Morad 1998). Diagenetic studies of carbonate rocks and of sandstone-shale systems commonly employ the $\delta^{18}O$ record of zoned carbonate cements to help constrain: (a) temperatures during different stages of sediment burial and cementation, (b) the evolution of pore water $\delta^{18}O$, (c) the pathways and timing of fluid/brine migration events and (d) the sources of cementing material (e.g., Arthur *et al.* 1983, Dutton and Land 1985, Longstaffe 1989, Fayek *et al.* 2001). The corresponding $\delta^{13}C$ values aid in identifying the source(s) of carbon (e.g., dissolved inorganic carbon in seawater versus carbon derived from different pathways of organic matter degradation/recycling by microbial communities).

The most abundant carbonate minerals in the rock record, and arguably the most commonly analysed in the above applications, are calcite/aragonite and compositions of the dolomite–ankerite series. Recent advances in the SIMS technique afford a new dimension to such studies by allowing isotopic records to be investigated *in situ* on the micrometre scale, provided that instrumental bias can be properly calibrated via the development and implementation of well-characterised, matrix-matched reference materials.

Experimental procedures

Overview of the methodological approach

We examined naturally occurring carbonate mineral samples with compositions along the dolomite–ankerite solution series and assessed the extent to which each was both chemically and isotopically ($\delta^{18}O$) homogenous. Over forty potential reference materials were evaluated to identify the thirteen $\delta^{18}O$ RMs reported here and used in the WiscSIMS Laboratory. A quantity (*ca.* 1–5 g) of each potential reference material was crushed and sieved to a grain size of 500–1000 μm. Clean grain separates were then prepared by handpicking under a binocular microscope. Twenty representative grains were chosen at random and made into grain mounts (see next section) and then evaluated first by BSE-SEM imaging (back-scattered electron, scanning electron microscopy). Those samples that exhibited only minimal or no contrast at maximum BSE-amplifier gain (i.e., minimal variations in mean atomic number) were chosen for further testing; they were evaluated semi-quantitatively by EDX-SEM (energy dispersive X-ray spectrometry) to identify desired compositions along the dolomite–ankerite series, and later by electron probe microanalysis (see section on EPMA below) for quantitative analysis of the cation chemistry (typically three analyses per each of twenty grains). SIMS $\delta^{18}O$ bias is expressed here in relation to the Fe# [= molar Fe/(Mg+Fe)] of dolomite–ankerite, as determined by EPMA. These materials were subsequently evaluated in terms of $\delta^{18}O$-variability on a scale of 10 μm by SIMS (instrumental configuration described below). The $\delta^{18}O$ value of each potential reference material was measured once from each of n = 20 grains; a potential reference material passed testing if the value of 2 standard deviations (2s) of those n = 20 measurements was < 0.3‰. Acceptance of materials for use as SIMS $\delta^{18}O$ reference materials was based on the following considerations. During calibration of the IMS 1280 instrument at WiscSIMS for work on minerals that exhibit solid solution behaviour, each reference material from the relevant suite of reference materials is measured four times (four different grains, once each) and an average 'raw' $\delta^{18}O$ value is calculated for use in determining the magnitude of instrumental bias in relation to chemical composition. Thus, an acceptable (and practical) SIMS $\delta^{18}O$ reference material for routine use, employing a 10 μm diameter spot size, is one for which the value of two standard deviations of n = 4 analyses varies by less

than ± 0.3‰ from spot to spot; this level of variability is expected based on considerations of instrument stability, counting statistics, as well as the sample-mount to sample-mount reproducibility of $\delta^{18}O$ values measured from a nominally homogenous material. For reference materials with slight heterogeneity, a 2*s* value of up to ± 0.5‰ was considered acceptable. Powdered aliquots of those materials that were accepted for use as reference materials were lastly analysed in triplicate by conventional phosphoric acid digestion and gas-source mass spectrometry to calibrate the $\delta^{18}O$ VSMOW value of each reference material (see section below).

Preparation of grain mounts

Grain mounts were prepared as 25-mm-diameter epoxy rounds (using Buehler EpoxyCure). All grains were placed within a radius of 5 mm from the geometrical centre of the mount so as to minimise any potential mass fractionation effects that have previously been observed near the edge of the sample holder. The raised lip of the sample holder covers the outer edge of the 25-mm epoxy round at a radial distance of 10 mm from the geometric centre of a normal holder (Kita *et al.* 2009), although new larger holders extend the uncovered sample surface to 11 mm (Peres *et al.* 2012). Several grains of calcite reference material UWC-3 (Kozdon *et al.* 2009) were positioned near the centre of each mount to serve as a drift monitor during calibration. The analytical surface was polished to a 0.25-μm finish using oil-based polycrystalline diamond suspensions (Buehler MetaDi Supreme) and Allied TECH-Cloth (chosen to help keep polishing relief to less than a few micrometres).

Compositional analysis by EPMA

Chemical analyses of the various dolomites and ankerites examined were performed using a CAMECA SX-51 instrument at the Cameron Electron Microprobe Laboratory (Department of Geoscience, University of Wisconsin-Madison). Data were collected during five analytical sessions; session-specific operating conditions, including the background correction methods employed and count rate acquisition times, are detailed in online supporting information Appendix S1. Care was taken to minimise beam-induced sample damage by defocussing the electron beam to either a 5 or 10 μm diameter. Damage of carbonate minerals during analysis can affect the stability and induce drift in characteristic fluorescent X-ray intensities; this was corrected by a feature in Probe for EPMA software (Donovan *et al.* 2007) called 'TDI' (time-dependent intensity), where data plotted in 'measured X-ray intensity' versus 'time' space are first detrended before the application of ZAF corrections.

The electron microprobe was standardised with the following reference materials for each of the cations determined: Delight dolomite (Ca, on a PET analyser crystal; Mg, TAP crystal), USNM 460 siderite (Fe, LiF crystal), rhodochrosite (Mn, LiF crystal) and strontianite (Sr, TAP crystal). Replicate measurements of the above reference materials were used to constrain the analytical precision during each session and to calculate the deviation between measured and accepted values (Appendix S1).

Grain mounts were coated with carbon (25 nm thickness) for EPMA; this carbon coat was subsequently removed prior to SIMS analysis, for which the sample surface was coated with a thin layer of gold to make it electrically conductive. Because part II of this study concerns the determination of carbon isotopes by SIMS, we were exceptionally careful in removing the carbon coat applied for EPMA; the grain mounts were repolished using a 0.25-μm oil-based polycrystalline diamond suspension, oils were removed by multiple alternating rinses in ethanol and de-ionised water (with brief ultrasound treatment), and each grain was individually inspected by reflected-light microscopy to verify that no remnants of the carbon coat were present.

Oxygen isotope determinations by SIMS

Oxygen isotope measurements were taken using a CAMECA IMS 1280 large radius multi-collector SIMS at the WiscSIMS Laboratory (Department of Geoscience, University of Wisconsin-Madison). The data set reported here was collected during multiple analytical sessions over a three-year period, employing both 10 and 3 μm diameter spot sizes. The example calibration curves that will be presented and discussed were constructed using data from session S12 (10 μm spot size) and session S14 (3 μm spot size).

Instrumental conditions during 10-μm-diameter spot sessions (sessions S1, S2, S6, S7, S9, S11, S12) were similar to those of Orland *et al.* (2009); a 10 keV, 1.3–1.4 nA primary beam of $^{133}Cs^+$ ions was focused to a ~ 10 μm diameter on the sample surface. The depth of sputtered sample pits was ~ 1 μm. Sample surfaces were made conductive by coating with a thin layer of gold (*ca.* 600 Å), and charge neutralisation was aided using an electron flood gun. The intensities (count-rates) of oxygen ions ($^{18}O^-$ and $^{16}O^-$) were collected simultaneously by two Faraday cup detectors (H1 and C, respectively), with a mass resolving power of 2500 for ^{18}O and ^{16}O. A typical intensity of $^{16}O^-$ ions was in the range of 2–3 × 10^9 cps (counts per

second). The duration of a single 10-μm spot measurement was ~ 4 min, which included an initial 10 s of pre-sputtering to remove the overlying gold coat, followed by an automated ~ 60 s routine that centred the secondary ion beam in the field aperture and optimised its transmission into the mass spectrometer, and lastly a collection period of 80 s for the $^{18}O^-$ and $^{16}O^-$ ion signals (twenty cycles of 4 s integrations).

In contrast to 10-μm-diameter spot sessions, instrumental conditions during the 3-μm session (S14) were similar to those reported in Kozdon *et al.* (2009) and Vetter *et al.* (2013). A 10 keV, 30 pA primary beam of $^{133}Cs^+$ ions was focused to a ~ 3 μm diameter on the sample surface, with a sputtering depth of 1–2 μm. Secondary $^{18}O^-$ and $^{16}O^-$ ion signals were detected simultaneously using an electron multiplier (H2) and a Faraday cup (L2), respectively. A typical count rate for $^{16}O^-$ ions was in the range of 3–5 × 10^7 cps. The duration of individual measurements during 3 μm spot size sessions was ~ 6.5 min, which included 120 s of pre-sputtering to remove the overlying gold coat, followed by an automated ~ 60 s routine that centred the secondary ion beam, and lastly a 200-s collection period for the $^{18}O^-$ and $^{16}O^-$ ion signals (twenty-five cycles of 8-second integrations).

Bulk $\delta^{18}O$ analysis by phosphoric acid digestion and gas-source mass spectrometry

Each potential reference material that proved to be suitably homogenous in $\delta^{18}O$ and cation composition was analysed by conventional phosphoric acid digestion and gas-source mass spectrometry (McCrea 1950) to determine its $\delta^{18}O$ value relative to the VSMOW scale. Approximately 25 mg of clean, representative grains were powdered using an agate mortar and pestle. Three ~ 5 mg aliquots were then digested at 100 °C for > 4 hr in '103%' phosphoric acid (D = 1.93; Rosenbaum and Sheppard 1986). The evolved CO_2 gas was cryogenically purified and analysed using a dual-inlet Finnigan/MAT 251 mass spectrometer. The O-isotope fractionation factor between $\delta^{18}O$ of the carbonate and $\delta^{18}O$ of the acid-extracted CO_2 was calculated using equation 4 of Rosenbaum and Sheppard (1986). The reference materials NBS 19 (calcite; Verkouteren and Klinedinst 2004) and/or (calcite) UWC-3 (Kozdon *et al.* 2009), calibrated to NBS 19, were measured as drift monitor materials with each batch of three replicates.

Results and discussion

The suite of SIMS $\delta^{18}O$ reference materials representing the dolomite–ankerite solid solution series consists of thirteen carbonate materials, ranging in composition from end-member dolomite to ankerite with a Fe# of 0.789 (Figure 1, Table 1). The range of calibrated $\delta^{18}O$ values represented by the suite extends from 9.19 to 22.60‰ VSMOW (Table 2; Appendix A). This article is accompanied by online supporting information appendices that contain (1) complete EPMA and SIMS data sets (Appendices S1–S4), (2) the error propagation associated with the construction of working calibration curves (Appendix S5), (3) a description of how sample analyses are corrected for SIMS $\delta^{18}O$ bias and the associated propagation of errors (Appendix S6), (4) additional examples of calibration curves (Appendix S7) and (5) an assessment of the reproducibility of our evaluation process of potential RMs (Appendix S8).

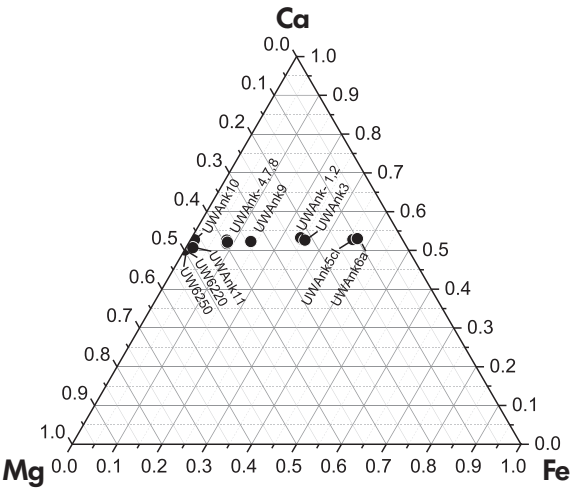

Figure 1. Carbonate Ca-Mg-Fe ternary diagram showing the range of compositions of UW dolomite–ankerite SIMS $\delta^{18}O$ calibration materials in this study.

Instrumental mass fractionation (i.e., bias) during the measurement of $\delta^{18}O$ reference materials is expressed by the formulation

$$\alpha^{18}O_{SIMS} = \frac{1 + (\delta^{18}O_{raw}/1000)}{1 + (\delta^{18}O_{VSMOW}/1000)} \qquad (1)$$

(after Kita *et al.* 2009), where '$\delta^{18}O_{raw}$' represents the background and detector dead-time (when electron multipliers are used) corrected $\delta^{18}O$ value of a reference material measured by SIMS; this value is expressed in conventional per mil notation (‰) and calculated relative to the $^{18}O/^{16}O$ ratio in VSMOW (i.e., normalised to $^{18}O/^{16}O_{VSMOW}$ = 0.00200520 ± 45; Baertschi 1976), but is not corrected for bias and is therefore not accurate relative to VSMOW. The '$\delta^{18}O_{VSMOW}$' term represents the average $\delta^{18}O$ value of the same reference material determined by conventional phosphoric acid digestion

Table 1.
Average chemical composition of each SIMS $\delta^{18}O$ RM in the dolomite-ankerite suite (by electron probe microanalysis)

Reference material	EPMA session i.d. and date	No. of grains	No. of EPMA analyses	Mg (mol %)	2s (%)	Ca (mol %)	2s (%)	Fe (mol %)	2s (%)	Mn (mol %)	2s (%)	Fe# [Fe/(Mg+Fe)]	2s	2SE	Fe (% m/m)	2s	2SE
UW6250	(S1) 2006 Sept.	15	15	49.80	1.00	50.10	1.00	0.20	0.20	–	–	0.004	0.005	0.001	0.05	0.15	0.04
UW6220	(S1) 2006 Sept.	15	15	49.66	1.00	50.23	1.00	0.20	0.10	–	–	0.004	0.004	0.001	0.06	0.11	0.03
UWAnk10	(S5a) 2014 Dec.	22	66	46.33	0.67	52.67	0.69	0.91	0.19	0.08	0.03	0.019	0.004	0.000	0.54	0.11	0.01
UWAnk11	(S5a) 2014 Dec.	20	60	47.62	1.98	50.51	2.06	1.54	0.38	0.25	0.46	0.031	0.008	0.001	0.91	0.23	0.03
UWAnk7	(S5b) 2014 Dec.	21	63	39.60	0.60	51.60	0.60	8.60	0.50	0.20	0.10	0.178	0.010	0.001	5.05	0.33	0.04
UWAnk8	(S5b) 2014 Dec.	19	57	38.80	1.90	52.00	0.90	8.00	0.70	1.20	0.60	0.171	0.019	0.003	4.69	0.42	0.06
UWAnk4	(S3) 2014 Mar.	20	30	38.84	2.90	51.46	2.90	8.46	1.00	1.24	0.50	0.179	0.020	0.004	4.93	0.57	0.10
UWAnk9	(S5b) 2014 Dec.	19	57	33.90	0.80	52.00	0.60	13.60	1.00	0.50	0.20	0.286	0.018	0.002	7.89	0.60	0.08
UWAnk1	(S2) 2012 July	22	22	22.11	1.70	52.03	1.00	24.10	2.00	1.72	1.00	0.522	0.038	0.008	13.58	1.21	0.26
UWAnk2	(S2) 2012 July	22	22	22.11	2.80	52.40	2.40	23.90	3.70	1.60	0.90	0.519	0.065	0.014	13.39	2.26	0.48
UWAnk3	(S3) 2014 Mar.	18	54	21.50	3.10	51.90	3.20	25.20	2.70	1.40	0.70	0.540	0.056	0.008	14.05	1.57	0.21
UWAnk5cl	(S4) 2014 July	20	61	10.76	1.70	51.44	1.50	35.27	2.00	2.54	0.60	0.766	0.034	0.004	19.16	1.41	0.18
UWAnk6a	(S4) 2014 July	22	68	9.66	1.90	51.64	2.00	36.09	2.60	2.61	0.60	0.789	0.041	0.005	19.56	1.69	0.20

and gas-source mass spectrometry and is expressed on the VSMOW scale (Vienna Standard Mean Ocean Water, Coplen 2011, Gonfiantini 1978, see Appendix A). Values can be converted to the VPDB scale (Vienna Pee-Dee Belemnite) using the equation of Coplen *et al.* (1983). Values of $\alpha^{18}O_{SIMS}$ are often close to unity; thus, for ease of comprehension in plotting such values on graphics and discussing them in-text, they are expressed using δ-notation in per mil (‰) and referred to as 'bias':

$$\text{bias}\,(‰) = 1000 \cdot (\alpha^{18}O_{SIMS}\text{-}1) \qquad (2)$$

Please note that while we make consistent use of δ-notation throughout this article, all equations have been set up such that all multiplication and/or division operations are always performed on α-terms (e.g., if two isotope ratio values that are expressed using δ-notation are to be multiplied or divided, they are first converted to α-values, then multiplied or divided, and subsequently converted back to values in δ-notation). We explicitly avoid the common approximation where $\delta_A - \delta_B \cong 1000\ln(\alpha_{A\text{-}B})$.

The values of bias for each of the $\delta^{18}O$ reference materials, calculated by Equation (2), are tabulated in Table 3 for multiple analytical sessions spanning a three-year period. Table 3 includes the averages of the measured $\delta^{18}O_{raw}$ values. The entire SIMS data set is provided in online supporting information (Appendices S2–S4).

Effect of Fe substitution on SIMS $\delta^{18}O$ bias in dolomite–ankerite

Calibration based on 10-µm spot data and a matrix bias correction: An example of a 10 µm diameter spot size calibration relating the magnitude of SIMS $\delta^{18}O$ bias to variation in cation chemistry of the dolomite–ankerite solid solution series is shown in Figure 2a. The discussion throughout this subsection concerns data from analytical session S12 (Table 3). During the calibration process leading up to the analysis of carbonate samples with compositions along the dolomite–ankerite series, the $\delta^{18}O$ bias of each reference material was expressed in relation (i.e., normalised) to the bias of the end-member dolomite reference material (UW6220) that was used to monitor instrument drift throughout the duration of the analytical session:

$$\text{bias}^*(\text{RM - UW6220}) = 1000 \cdot \left[\frac{1 + (\text{bias}_{RM}/1000)}{1 + (\text{bias}_{UW6220}/1000)}\text{-}1\right] \qquad (3)$$

The associated propagation of errors is derived in Appendix S5. Several grains of the drift monitor material

Table 2.
Measured extent of $\delta^{18}O$ homogeneity in RMs of the dolomite-ankerite suite (by SIMS; spot size = 10 μm)

Reference material	Fe# [Fe/(Mg+Fe)]	Source locality	SIMS session i.d. and date	No. of grains	No. of SIMS analyses	True[a] $\delta^{18}O$ (‰, VSMOW)	SIMS 2*s*	SIMS 2SE
UW6250	0.004	Thornwood, Westchester County, New York, USA	(SD1) 2006. Sept.	14	16	21.40	0.31	0.08
UW6220	0.004	Tuckahoe, Westchest County, New York, USA	(SD1) 2006. Sept.	15	17	22.60	0.30	0.07
UWAnk10	0.019	St. Johnsville, Montgomery County, New York, USA	(S12) 2014. Dec.	20	20	19.55	0.32	0.07
UWAnk11[b]	0.031	Balmer County, Maryland, USA	(S12) 2014. Dec.	20	30	10.49	0.75	0.14
UWAnk7	0.179	near Selåsvann, Aust-Agder, Norway	(S12) 2014.Dec.	21	21	11.38	0.37	0.08
UWAnk8	0.171	Quincy/Salem Neck, Norfolk/Essex Counties, Massachusetts, USA	(S12) 2014. Dec.	19	20	9.19	0.29	0.07
UWAnk4	0.179	Quincy/Salem Neck, Norfolk/Essex Counties, Massachusetts, USA	(S6) 2014. Apr.	15	20	9.22	0.46	0.10
UWAnk4[c]	0.179	Quincy/Salem Neck, Norfolk/Essex Counties, Massachusetts, USA	(S9) 2014. Aug.	16	18	9.22	0.34	0.08
UWAnk9	0.286	near town of Llallagua, Potosi Dept., Bolivia	(S12) 2014. Dec.	19	25	11.68	0.40	0.08
UWAnk1	0.522	Pulaski County, Arkansas, USA	(SD2) 2012. July	22	24	15.87	0.44	0.09
UWAnk2	0.519	Pulaski County, Arkansas, USA	(SD2) 2012. July	22	23	15.90	0.45	0.09
UWAnk3	0.539	Pulaski County, Arkansas, USA	(S6) 2014. Apr.	18	20	15.82	0.35	0.08
UWAnk5 cl	0.766	Erzberg Mine, near town of Eisenerz, Styria, Austria	(S9) 2014. Aug.	20	24	17.11	0.33	0.07
UWAnk6a	0.789	Erzberg Mine, near town of Eisenerz, Styria, Austria	(S9) 2014. Aug.	22	22	15.99	0.51	0.11

[a] $\delta^{18}O$ VSMOW value determined by conventional phosphoric acid digestion and gas-source mass spectrometry (see Appendix A).
[b] This RM may be used for calibration only if analysed repeatedly a sufficient number of times to drive the standard error (at the 95% confidence level) below 0.15‰ (approx. $n = 10$).
[c] Orientation effect test; see text.

were comounted with samples, and each batch of ten sample measurements was 'bracketed' by eight analyses of this material. Thus, by systematically measuring the drift monitor material throughout the analytical session, instrumental drift could be corrected and the $\delta^{18}O$ bias of each sample-spot measurement (Appendix S6) could be appropriately scaled to the instrumental conditions at the time of calibration.

The distribution of reference material data points in relation to one another in the plot of bias*(RM-UW6220) versus Fe# (Figure 2a) can be expressed using the Hill equation [Equation (4); e.g., review of Goutelle *et al.* 2008], which has wide-ranging applicability in describing empirical relationships of the 'component concentration' versus 'measured effect' type, especially for systems that behave non-linearly and reach saturation:

$$\text{bias}^*(\text{RM-UW6220}) = \frac{(\text{bias}^*_{max})x^n}{k^n + x^n}(\text{matrix bias correction}) \quad (4)$$

where '*x*' is the Fe# (based on EPMA data), '*n*' is a sigmoidicity factor and '*k*' = *x* (Fe#) at the value of ½ bias*$_{max}$. For a hypothetical data set where the function saturates as *x* approaches 1 (rather than being asymptotic, as in this case), the term 'bias*$_{max}$' would represent the maximum observed bias*(RM-UW6220) in the suite of reference materials measured during a particular analytical session. The bias*(RM-UW6220) value on the left-hand side of Equation (4) is calculated using Equations (1–3). Note that in this application, Equation (4) can only be defined for $0 \leq x \leq 1$, that is it is constrained by the physical limits of solid solution. The reference material data for session 12 (Table 3) was fitted using OriginPro (v.9.0) software, yielding

Table 3.
SIMS $\delta^{18}O$ bias data for dolomite–ankerite reference materials measured during multiple analytical sessions over a three-year period (2012–2015)

Reference material	Fe#[a]	$\delta^{18}O$ True[b] (‰, VSMOW)	Session 14, 2015. Jan. (spot-size = 3 µm)			Session 12, 2014. Dec. (spot-size = 10 µm)			Session 11, 2014. Oct. (spot-size = 10 µm)			Session 9, 2014. Aug. (spot-size = 10 µm)			Session 7, 2014. May (spot-size = 10 µm)			Session D2, 2012. July (Spot-size = 10 µm)		
			$\delta^{18}O$ raw[c] (‰)	$\delta^{18}O$ bias[c,d] (‰)	$\delta^{18}O$ bias* (RM-UW6220)[e]	$\delta^{18}O$ raw[c] (‰)	$\delta^{18}O$ bias[c,d] (‰)	$\delta^{18}O$ bias* (RM-UW6220)[e]	$\delta^{18}O$ raw[c] (‰)	$\delta^{18}O$ bias[c,d] (‰)	$\delta^{18}O$ bias* (RM-UW6220)[e]	$\delta^{18}O$ raw[c] (‰)	$\delta^{18}O$ bias[c,d] (‰)	$\delta^{18}O$ bias* (RM-UW6220)[e]	$\delta^{18}O$ raw[c] (‰)	$\delta^{18}O$ bias[c,d] (‰)	$\delta^{18}O$ bias* (RM-UW6220)[e]	$\delta^{18}O$ raw[c] (‰)	$\delta^{18}O$ bias[c,d] (‰)	$\delta^{18}O$ bias* (RM-UW6220)[e]
UW6250	0.004	21.40	-1.01	-21.94	**-0.46**	7.54	-13.57	**0.06**	–	–	–	–	–	–	–	–	–	–	–	–
UW6220	0.004	22.60	0.62	-21.49	**0**	8.66	-13.63	**0**	10.98	-11.36	0	12.36	-10.02	0	10.87	-11.47	0	8.35	-13.94	0
UWAnk10	0.019	19.55	-1.13	-20.28	**1.24**	7.35	-11.97	**1.68**	–	–	–	–	–	–	–	–	–	–	–	–
UWAnk11	0.031	10.49	-9.69	-19.97	**1.56**	-1.23	-11.60	**2.06**	–	–	–	–	–	–	–	–	–	–	–	–
UWAnk7	0.179	11.38	-2.61	-13.83	**7.83**	5.46	-5.85	**7.88**	–	–	–	–	–	–	–	–	–	–	–	–
UWAnk8	0.171	9.19	-5.07	-14.13	**7.52**	3.24	-5.90	**7.83**	–	–	–	–	–	–	–	–	–	–	–	–
UWAnk4	0.179	9.22	-4.79	-13.88	**7.77**	3.21	-5.96	**7.77**	5.11	-4.08	7.37	5.85	-3.34	6.75	4.61	-4.57	6.97	–	–	–
UWAnk4[f]	0.179	9.22	–	–	–	–	–	–	–	–	–	5.69	-3.50	6.58	–	–	–	–	–	–
UWAnk9	0.286	11.68	-1.81	-13.34	**8.33**	6.49	-5.13	**8.61**	–	–	–	–	–	–	–	–	–	–	–	–
UWAnk1	0.522	15.87	3.44	-12.25	**9.45**	12.48	-3.34	**10.43**	13.81	-2.03	9.44	14.23	-1.61	8.49	13.08	-2.74	8.83	10.70	-5.08	8.98
UWAnk2	0.519	15.90	–	–	–	–	–	–	–	–	–	–	–	–	–	–	–	10.91	-4.92	9.15
UWAnk3	0.539	15.82	3.83	-11.81	**9.90**	–	–	–	–	–	–	–	–	–	–	–	–	–	–	–
UWAnk5cl	0.766	17.11	5.80	-11.12	**10.60**	14.16	-2.90	**10.88**	16.03	-1.06	10.42	16.58	-0.52	9.59	–	–	–	–	–	–
UWAnk6a	0.789	15.99	4.59	-11.22	**10.50**	12.68	-3.26	**10.51**	14.50	-1.47	10.00	15.24	-0.74	9.37	–	–	–	–	–	–

[a] Fe# = molar Fe/(Mg+Fe); the uncertainties that accompany this EPMA-derived parameter are tabulated in Table 1.
[b] $\delta^{18}O$ VSMOW value determined by conventional phosphoric acid digestion and gas-source mass spectrometry (see Appendix A).
[c] Value corrected for instrumental drift relative to UWC-3 Reference Bracket (session specific; see Appendix S2).
[d] Value calculated using Equations (1) and (2).
[e] Value calculated using Equation (3).
[f] Alternative mount used to assess potential orientation effects; see text.

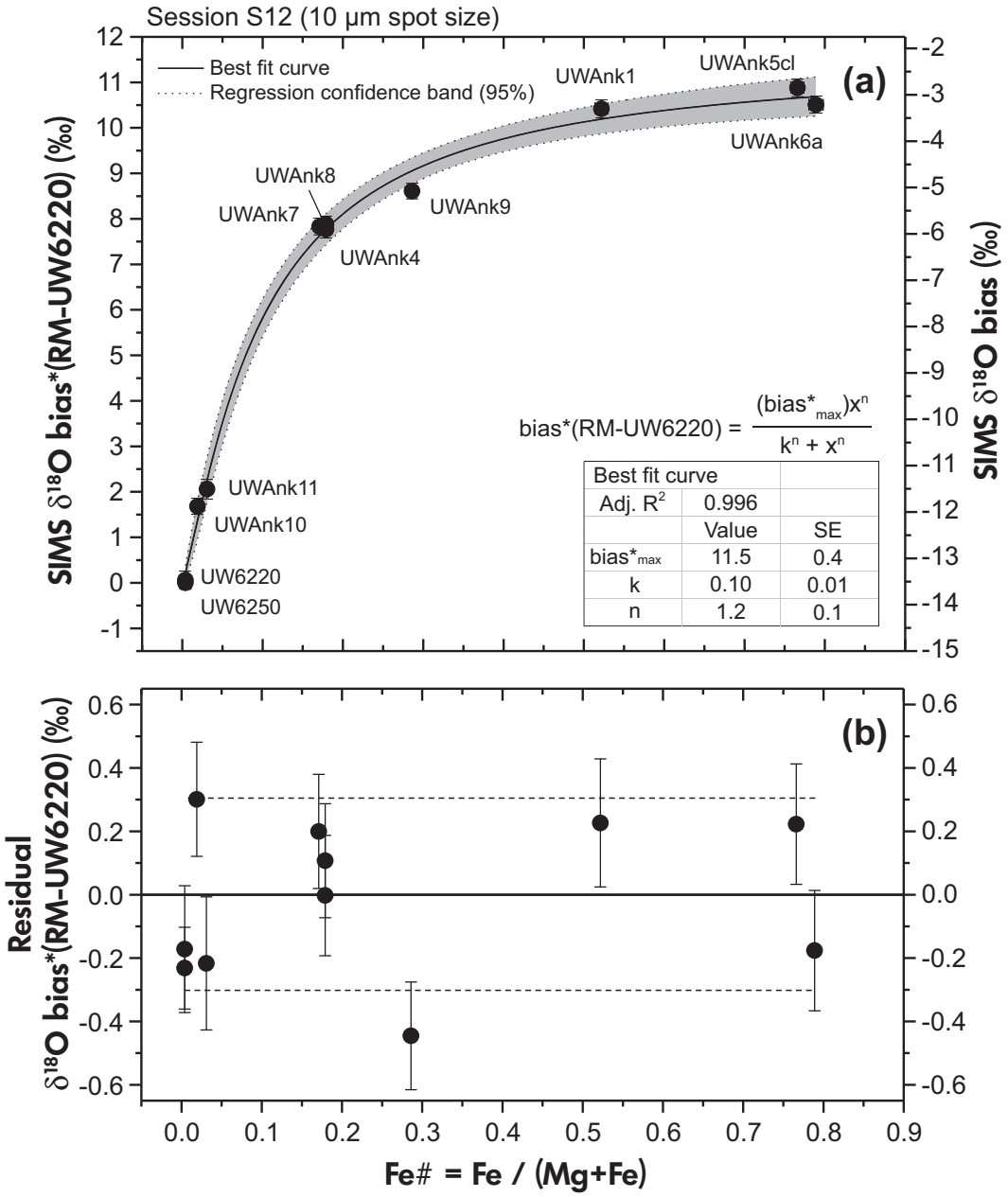

Figure 2. (a) Plot relating SIMS $\delta^{18}O$ bias (‰) to the cation composition of the dolomite–ankerite solid solution series [Fe# = Fe/(Mg+Fe)] for a typical calibration using a 10 µm diameter spot size. The sample matrix effect can be accurately estimated using the Hill equation, which is commonly employed to describe relations of 'concentration' versus 'measured effect' type, especially in systems that behave non-linearly and reach saturation. (b) Plot of the calibration residual. For most reference materials in the suite, the averaged measured value of $\delta^{18}O$ bias*(RM-UW6220) differs by < 0.3‰ from the value predicted by the calibration (depicted by solid lines).

the following best-fit values for the three parameters of the Hill equation: $n = 1.2 \pm 0.1$, $k = 0.10 \pm 0.01$, $bias^*_{max} = 11.5 \pm 0.4$ (uncertainties are standard errors; adjusted $R^2 = 0.996$; Figure 2a). For most reference materials in the suite, the averaged measured value of $\delta^{18}O$ bias*(RM-UW6220) differs by < 0.3‰ from the value predicted by the calibration model; this is a measure of the accuracy of the matrix bias correction in relation to the $\delta^{18}O$ VSMOW values determined for the suite of reference materials by conventional phosphoric acid digestion and gas-source mass spectrometry (Appendix A).

The measured SIMS $\delta^{18}O$ bias for the dolomite–ankerite series was greatest for end-member dolomite and decreased

exponentially by ~ 10‰ with increasing Fe# (Figure 2a). Note the two different vertical axes of Figure 2a; the right-hand axis represents $\delta^{18}O$ bias (‰) values that were corrected for instrument drift but that were not normalised to the UW6220 drift monitor material (i.e., values that represent the per mil difference between $\delta^{18}O_{raw}$ and $\delta^{18}O_{VSMOW}$). The left-hand axis of Figure 2a represents the working calibration curve, where the $\delta^{18}O$ bias of each dolomite–ankerite reference material is normalised to the bias of the end-member dolomite drift monitor material (i.e., bias*(RM-UW6220)). Because of the extreme curvature of the bias* (RM-UW6220) versus Fe# relation, careful corrections are necessary for analyses of unknown samples with chemical compositions near that of end-member dolomite. The bias correction is greatest for the first one mole % Fe (i.e., for the first ~ 0.55% *m/m* Fe, or Fe# = 0.02); failure to correct Fe# = 0.02 results in an error of 1.5‰, which increases to 3.5‰ for Fe# = 0.05 (Figure 2a, Table 3). The dolomite–ankerite series is commonly subdivided into non-ferroan dolomite (Fe# 0.0–0.1), ferroan dolomite (Fe# 0.1–0.2) and ankerite (Fe# > 0.2) (Chang *et al.* 1996). Employing this scheme, the bias*(RM-UW6220) correction (a) changes most rapidly (by ~ 6‰) in the narrow compositional range of the 'non-ferroan' dolomite field, (b) changes more gradually (by another ~ 2‰ from 6 to 8‰) in the equally narrow compositional range of 'ferroan dolomite' and finally (c) tapers off, changing by only an additional ~ 3‰ throughout the more extended compositional range of ankerite.

The molar abundance of Mn in the suite of reference materials varies from 0 to 2.61% (Mn/(Ca+Mg+Fe+Mn); Table 1). However, despite the similar physical properties of the Mn^{2+} and Fe^{2+} cations and their largely shared preference for the same structural site in the crystal lattice (Reeder and Dollase 1989), this amount of Mn^{2+} substitution appears to have had no comparable effect to that of Fe^{2+} at similar concentrations (between Fe# 0.0–0.2) on the measured SIMS $\delta^{18}O$ bias*(RM-UW6220). The variance of mol % Mn was uncorrelated to the residual of the matrix bias calibration (R^2 = 0.07, 95% confidence limit). This was further assessed by treating Fe^{2+} and Mn^{2+} as a single species with regard to the effect on bias [i.e., (Fe+Mn)/(Fe+Mn+Mg)] and evaluating whether the quality of the Hill fit would improve (or degrade). No significant improvement was observed, with the value of the calibration residual remaining unchanged (compare Figure 2 and Appendix S7a). Work is currently in progress on the development of an end-member kutnohorite reference material [$CaMn(CO_3)_2$; also a member of the dolomite group] to comprehensively assess the effect of Mn^{2+} substitution on $\delta^{18}O$ bias in relation to end-member dolomite. The molar abundance of Ca in the suite of reference materials also varies slightly [50–52.5 mol % Ca/(Ca+Mg+Fe+Mn); Table 1], although this variance was likewise uncorrelated to the residual of the matrix bias calibration (R^2 = 0.28, 95% confidence limit). Thus, no secondary matrix corrections needed to be implemented for small variability in Ca or Mn.

Calibration based on 3 μm spot size measurements: An example of a 3 μm spot size calibration relating bias*(RM-UW6220) to the Fe# of the dolomite-ankerite series is shown in Figure 3a; the discussion throughout this subsection concerns data from session S14 and how it compares with data from session S12 (the 10 μm spot size calibration; Table 3). The measured $\delta^{18}O$ bias (not normalised to the UW6220 drift monitor material) was again greatest for end-member dolomite, although its magnitude was ~ 10‰ larger when using a 3 μm spot size in comparison with the calibration employing a 10-μm-diameter spot (Table 3). However, the difference in the value of bias*(RM-UW6220) between the extreme ends of the calibration (i.e., between end-member dolomite UW6220 and ankerite UWAnk6a) was similar to the 10-μm spot calibration at ~ 10.5‰. In modelling the curvature of the bias*(RM-UW6220) versus Fe# trend of the 3-μm calibration, the best-fit values of the '*n*' and '*k*' Hill equation parameters (1.4 ± 0.1, *k* = 0.10 ± 0.01) were within fitting error of those for the trend of the 10 μm calibration (session S12 data; compare Figure 2a and Appendix S7b). Thus for simplicity, the same parameter values (from 10-μm session S12) were applied in constructing the 3-μm working calibration curve (yielding an adjusted R^2 value of 0.994; compare Figures 2a and 3a). However, note that whereas the spot-to-spot repeatability was typically within ± 0.3‰ (2*s*) for measurements employing a spot size of 10 μm, the precision decreased to ± 0.7‰ (2*s*) for spot diameters of 3 μm. For most RMs in the suite, the averaged measured value of $\delta^{18}O$ bias*(RM-UW6220) differed by < 0.4‰ from the value predicted by the 3-μm calibration model.

Constancy of the Hill fit throughout multiple sessions

It is common for SIMS analyses that the instrument bias varies from session to session. This was observed for the suite of dolomite–ankerite reference materials in this study, where the magnitude of both bias and bias*(RM-UW6220) changed by up to several ‰ between different measurement sessions (Table 3); this is reflected by the best-fit value of the '$bias^*_{max}$' parameter of the Hill equation. Despite this, we found that the overall distribution of reference material data points in relation to one another in plots of bias*(RM-UW6220) versus Fe# was remarkably consistent. For

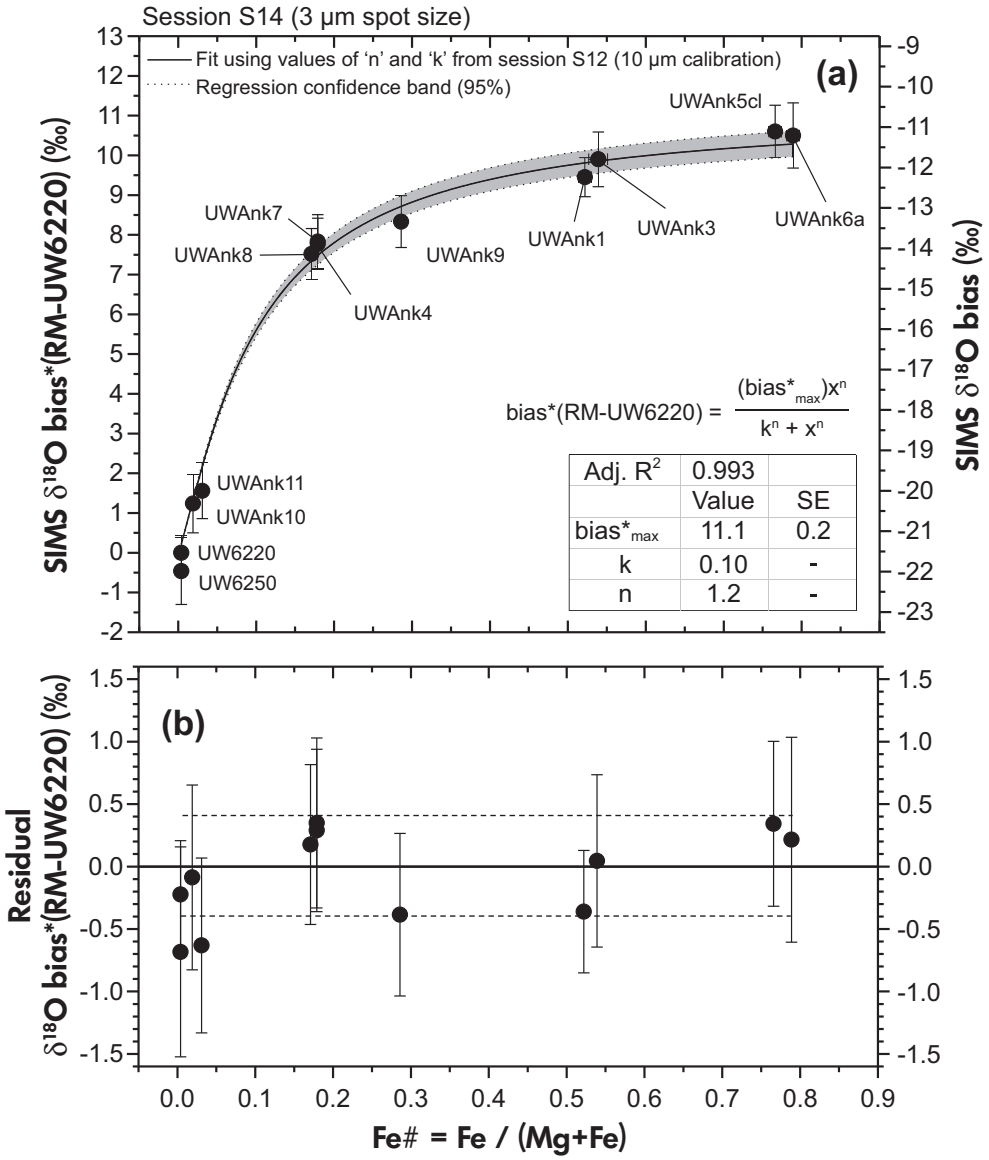

Figure 3. (a) Plot relating SIMS $\delta^{18}O$ bias (‰) to the cation composition of the dolomite–ankerite solid solution series [Fe# = Fe/(Mg+Fe)] for a typical calibration using a spot size 3 µm in diameter. The sample matrix effect can be accurately estimated using the same model parameters as in the 10 µm spot size calibration (see Figure 2). (b) Plot of the calibration residual. For most reference materials in the suite, the averaged measured value of $\delta^{18}O$ bias*(RM-UW6220) differed by < 0.4‰ from the value predicted by the calibration (depicted by solid lines).

example, the values of the Hill equation shape parameters '*n*' and '*k*' determined for the full suite of reference materials during session S12 (with $n = 1.2$, $k = 0.10$) can be used as constants to fit a trend to calibrations from past analytical sessions (e.g., sessions S11, S9, S7, Appendix S7c–e), allowing only the '$bias^*_{max}$' parameter to vary in response to session-specific conditions. In each case, the outcome was indistinguishable from modelling scenarios where all three parameters '*n*', '*k*' and '$bias^*_{max}$' were allowed to vary in the optimisation algorithm; for each of the past analysis sessions, the averaged measured value of $\delta^{18}O$ bias*(RM-UW6220) differed by < 0.3‰ from the value predicted by the session S12 10-µm calibration model (Appendix S7c–e). In effect, the '$bias^*_{max}$' parameter behaves as an analytical session-specific scaling factor. We found that various equations, for example exponential functions (which appear as a reasonable first choice for fitting the reference material data), did not provide the same degree of flexibility as the Hill equation in this regard; that is, more than a single parameter needed to be varied to achieve a reasonable fit to reference material data from past analytical sessions. More importantly, however, various exponential fits yielded asymmetric residuals

that were up to twice as large for some (but not all) reference materials compared with the Hill function model. It is important to point out, however, that this best-fit Hill function (with n = 1.2 and k = 0.10) is an empirical observation for data from the IMS 1280 instrument and tuning protocols at the WiscSIMS laboratory. Other laboratories will need to calibrate their own parameters by analysis of multiple carbonate reference materials.

Assessment of crystallographic orientation effects on measured $\delta^{18}O$ bias*(RM-UW6220)

It has been shown for magnetite and a few other oxide minerals that the instrument bias for SIMS $\delta^{18}O$ measurements varies systematically according to the angular relation of the primary and secondary beams to the crystal structure of the sample (Huberty *et al.* 2010, Kita *et al.* 2011). Measureable orientation effects have not been seen for calcite or any silicate mineral, but dolomite–ankerites have not been previously investigated in detail. In the preparation of grain mounts, rhombs of dolomite–ankerite have a strong tendency to be preferentially oriented with the {101} cleavage plane parallel to the sample casting plate (hence to the eventual analytical surface). The randomness of the rotational positioning of the cleavage face parallel to the sample surface does diversify the number of unique crystallographic orientations that will be exposed during SIMS measurements, but does not allow for an assessment as to whether the SIMS $\delta^{18}O$ bias could differ significantly in the case where the rhomb body-diagonal long axis is orthogonal to the analytical surface. To test this, we prepared an alternative mount containing grains of reference material UWAnk4 (n = 15); the long rhomb body-diagonal axis of each grain was pressed into a narrow trough cut into several layers of carbon tape to maintain an approximately orthogonal orientation to the sample casting plate during preparation. The values of bias*(UWAnk4-UW6220) were determined for both mounts during the same analytical session (session S9, Table 3) and were well within the ± 0.3‰ 2s uncertainty of the reference material UWC-3 used to monitor instrument drift (6.75‰ versus 6.58‰; Table 3). Thus, there was no measureable difference in bias for the different crystallographic orientations of ankerite in these mounts.

Implications for carbonate studies and concluding remarks

We have demonstrated the highly non-linear nature of SIMS instrumental bias on $\delta^{18}O$ measured from carbonate minerals with compositions along the dolomite–ankerite solid solution. With the routine configuration and tuning conditions of the IMS 1280 for carbonate mineral analysis at WiscSIMS, the $\delta^{18}O$ bias decreased exponentially by ~ 10‰ with increasing Fe content [i.e., the Fe# = Fe/(Mg+Fe)] in dolomite–ankerite. Bias was accurately modelled using the Hill equation, which reproduced reference material data from routine 10 μm spot size analytical sessions to within 0.3‰ in relation to the certified reference material NBS 19 (Verkouteren and Klinedinst 2004). The uncertainty associated with differences in Fe# was of similar magnitude to the typical spot-to-spot repeatability (precision) assigned to individual sample-spot analyses (± 0.3‰ at 2s) based on replicate analyses (n = 8) of the drift monitor material that 'bracketed' each set of ten sample measurements. Adding these terms in quadrature indicates that the accuracy of these analyses was ~ ± 0.5‰ (2s) relative to NBS 19 if there are no additional sources of error.

Given the importance of the determination of $\delta^{18}O$ (and $\delta^{13}C$) in carbonates in the geosciences, especially in the fields of reconstructing past climatic conditions throughout the evolution of the Earth system and of the early Martian environment, we call attention to the need for further basic research in empirically constraining SIMS matrix effects for common carbonate compositions. While the $\delta^{18}O$ bias is approximately linear from calcite to dolomite to magnesite (Valley and Kita 2009, Rollion-Bard and Marin-Carbonne 2011), a partial data set indicates that the bias between magnesite and siderite is highly non-linear (Valley and Kita 2009). For the analysis of sample materials with compositions that are not constrained to the binary joins of the Ca–Mg–Fe carbonate ternary plot and in which substantial Mn substitution is observed (such as carbonates in the Martian meteorite ALH 84001), a more comprehensive, multivariate approach is needed to accurately contour the bias landscape as it changes in relation to cation chemistry.

Acknowledgements

This research was supported by the U.S. Department of Energy Office of Science, Office of Basic Energy Sciences under Award Number DE-FG02-93ER14389. WiscSIMS is partly supported by the U.S. National Science Foundation (EAR-1355590). KK and JWV were also supported by the NASA Astrobiology Institute. We thank our colleagues at UW-Madison: Noriko Kita for many constructive discussions and SIMS support, Jim Kern for SIMS support and Phil Gopon for assistance with SEM. We thank B.C. Schreiber and M. Harrell (both at the University of Washington) for help in acquiring sample material that became reference material UWAnk8. The ankerite specimen that became reference material UWAnk4 was provided by the Smithsonian Institution (USNM number 93418). We thank Rick Hervig and Richard Stern for constructive reviews of this work.

References

Ahlbrandt T.S., Charpentier R.R., Klett T.R., Schmoker J.W., Schenk C.J. and Ulmishek G.F. (2005)
Global resource estimates from total petroleum system. American Association of Petroleum Geologists Memoir, 86, 324 pp.

Arthur M.A., Anderson T.F., Kaplan I.R., Veizer J. and Land L.S. (1983)
Stable isotopes in sedimentary geology. Society of Economic Paleontologists and Mineralogists, Short Course No. 10 (Dallas).

Baertschi P. (1976)
Absolute ^{18}O content of standard mean ocean water. Earth and Planetary Science Letters, 31, 341–344.

Baumgartner L.P. and Valley J.W. (2001)
Stable isotope transport and contact metamorphic fluid flow. In: Valley J.W. and Cole D.R. (eds), Stable isotope geochemistry. Reviews in Mineralogy and Geochemistry, 43, 415–468.

Blatt H. and Jones R.L. (1975)
Proportions of exposed igneous, metamorphic, and sedimentary rocks. Geological Society of America Bulletin, 81, 255–262.

Bowman J.R., Valley J.W. and Kita N.T. (2009)
Mechanisms of oxygen isotopic exchange and isotopic evolution of $^{18}O/^{16}O$-depleted periclase zone marbles in the Alta aureole, Utah: Insights from ion microprobe analysis of calcite. Contributions to Mineralogy and Petrology, 157, 77–93.

Buick R. (2003)
Life in the Archaean. In: Briggs D.E.G. and Crowther P.R. (eds), Palaeobiology II. Blackwell Publishing (Oxford), 13–21.

Chang L.L.Y., Howie R.A. and Zussman J. (1996)
Rock-forming minerals, Volume 5B: Non-silicates: Sulphates, carbonates, phosphates and halides. Longman (Harlow, Essex), 383pp.

Coplen T.B. (2011)
Guidelines and recommended terms for expression of stable-isotope-ratio and gas-ratio measurement results. Rapid Communications in Mass Spectrometry, 25, 2538–2560.

Coplen T.B., Kendall C. and Hopple J. (1983)
Comparison of stable isotope reference samples. Nature, 302, 236–238.

Donovan J.J., Kremser D. and Fournelle J.H. (2007)
Probe for Windows user's guide and reference (Enterprise edition). Probe Software Incorporated (Eugene, Oregon), 355pp.

Dutton S.P. and Land L.S. (1985)
Meteoric burial diagenesis of Pennsylvanian arkosic sandstones, south-western Anadarko Basin, Texas. American Association of Petroleum Geologists Bulletin, 69, 22–38.

Eiler J.M., Graham C. and Valley J.W. (1997)
SIMS analysis of oxygen isotopes: Matrix effects in complex minerals and glasses. Chemical Geology, 138, 221–244.

Eiler J.M., Valley J.W., Graham C.M. and Fournelle J. (2002)
Two populations of carbonate in ALH84001: Geochemical evidence for discrimination and genesis. Geochimica et Cosmochimica Acta, 66, 1285–1303.

Fayek M., Harrison M., Grove M., McKeegan K.D., Coath C.D. and Boles J.R. (2001)
In situ stable isotopic evidence for protracted and complex carbonate cementation in a petroleum reservoir, North Coles Levee, San Joaquin Basin, California, U.S.A. Journal of Sedimentary Research, 71, 444–458.

Ferry J.M., Kitajima K., Strickland A. and Valley J.W. (2014)
Ion microprobe survey of grain-scale oxygen isotope geochemistry of minerals in metamorphic rocks. Geochimica et Cosmochimica Acta, 144, 403–433.

Fitzsimons I.C.W., Harte B. and Clark R.M. (2000)
SIMS stable isotope measurement: Counting statistics and analytical precision. Mineralogical Magazine, 64, 59–83.

Gonfiantini R. (1978)
Standards for stable isotope measurements in natural compounds. Nature, 271, 534–536.

Goutelle S., Maurin M., Rougier F., Barbaut X., Bourguignon L., Ducher M. and Maire P. (2008)
The Hill equation: A review of its capabilities in pharmacological modelling. Fundamental and Clinical Pharmacology, 22, 633–648.

Hervig R.L., Williams P., Thomas R.M., Schauer S.N. and Steele I.M. (1992)
Microanalysis of oxygen isotopes in insulators by secondary ion mass spectrometry. International Journal of Mass Spectrometry and Ion Process, 120, 45–63.

Holland G., Saxton J.M., Lyon I.C. and Turner G. (2005)
Negative $\delta^{18}O$ values in Allan Hills 84001 carbonate: Possible evidence for water precipitation on Mars. Geochimica et Cosmochimica Acta, 69, 1359–1370.

Huberty J.M., Kita N.T., Kozdon R., Heck P.R., Fournelle J.H., Spicuzza M.J., Xu H. and Valley J.W. (2010)
Crystal orientation effects on instrumental bias of $\delta^{18}O$ in magnetite by SIMS. Chemical Geology, 276, 269–283.

Ickert R. and Stern R.A. (2013)
Matrix corrections and error analysis in high-precision SIMS $^{18}O/^{16}O$ measurements of Ca–Mg–Fe garnet. Geostandards and Geoanalytical Research, 37, 429–448.

references

Jaffrés J.B.D., Shields G.A. and Wallmann K. (2007)
The oxygen isotope evolution of seawater: A critical review of a long-standing controversy and an improved geological water cycle model for the past 3.4 billion years. Earth-Science Reviews, 83, 83–122.

Kita N.T., Ushikubo T., Fu B. and Valley J.W. (2009)
High precision SIMS oxygen isotope analysis and the effect of sample topography. Chemical Geology, 264, 43–57.

Kita N.T., Huberty J.M., Kozdon R., Beard B.L. and Valley J.W. (2011)
High precision SIMS oxygen, sulfur and iron stable isotope analyses of geological materials: Accuracy, surface topography and crystal orientation. SIMS XVII Proceedings, Surface and Interface Analysis, 43, 427–431.

Kozdon R., Ushikubo T., Kita N.T., Spicuzza M. and Valley J.W. (2009)
Intratest oxygen isotope variability in the planktonic foraminifer *N. pachyderma*: Real versus apparent vital effects by ion microprobe. Chemical Geology, 258, 327–337.

Kozdon R., Kelly D.C., Kita N.T., Fournelle J.H. and Valley J.W. (2011)
Planktonic foraminiferal oxygen isotope analysis by ion microprobe technique suggests warm tropical sea surface temperatures during the Early Paleogene. Paleoceanography, 26, 1–17.

Leshin L.A., McKeegan K.D., Carpenter P.K. and Harvey R.P. (1998)
Oxygen isotopic constraints on the genesis of carbonates from Martian meteorite ALH84001. Geochimica et Cosmochimica Acta, 62, 3–13.

Longstaffe F.J. (1989)
Stable isotopes as tracers in clastic diagenesis. In: Hutcheon I.E. (ed.), Burial diagenesis. Mineralogical Association of Canada Short Course Handbook, 15, 201–277.

McCrea J.M. (1950)
On the isotopic chemistry of carbonates and a paleotemperature scale. Journal of Chemical Physics, 18, 849–857.

Morad S. (1998)
Carbonate cementation in sandstones: Distribution patterns and geochemical evolution. In: Morad S. (ed.), Carbonate cementation in sandstones. International Association of Sedimentologists Special Publication, 26, 1–26.

Orland I.J., Bar-Matthews M., Kita N.T., Ayalon A., Matthews A. and Valley J.W. (2009)
Climate deterioration in the Eastern Mediterranean as revealed by ion microprobe analysis of a speleothem that grew from 2.2 to 0.9 ka in the Soreq Cave, Israel. Quaternary Research, 71, 27–35.

Peres P., Kita N.T., Valley J.W., Fernandes F. and Schuhmacher M. (2012)
New sample holder geometry for high precision isotope analyses. Surface and Interface Analysis (SIMS Proceedings), 45, 553–556.

Prokoph A., Shields G.A. and Veizer J. (2008)
Compilation and time-series analysis of marine carbonate $\delta^{18}O$, $\delta^{13}C$, $^{87}Sr/^{86}Sr$ and $\delta^{34}S$ databases through Earth history. Earth-Science Reviews, 87, 113–134.

Reeder R.J. and Dollase W.A. (1989)
Structural variation in the dolomite–ankerite solid-solution series: An X-ray, Mössbauer, and TEM study. American Mineralogist, 74, 1159–1167.

Riciputi L.R., Paterson B.A. and Ripperdan R.L. (1998)
Measurement of light stable isotope ratios by SIMS: Matrix effects for oxygen, carbon, and sulfur isotopes in minerals. International Journal of Mass Spectrometry, 178, 81–112.

Rollion-Bard C. and Marin-Carbonne J. (2011)
Determination of SIMS matrix effects on oxygen isotopic compositions in carbonates. Journal of Analytical Atomic Spectrometry, 26, 1285–1289.

Rosenbaum J. and Sheppard S.M.F. (1986)
An isotopic study of siderites, dolomites and ankerites at high temperatures. Geochimica et Cosmochimica Acta, 50, 1147–1150.

Shaheen R., Niles P.B., Chong K., Corrigan C.M. and Thiemens M.H. (2015)
Carbonate formation events in ALH 84001 trace the evolution of the Martian atmosphere. Proceedings of the National Academy of Sciences, 112, 336–341.

Tucker M.E. (2001)
Sedimentary petrology (3rd edition). Blackwell Science (Oxford), 262pp.

Tucker M.E. and Wright V.P. (1990)
Carbonate sedimentology. Blackwell Science (Oxford), 482pp.

Valley J.W. and Kita N.T. (2009)
In situ oxygen isotope geochemistry by ion microprobe. In: Fayek M. (ed.), Secondary ion mass spectrometry in the Earth sciences. Mineralogical Association of Canada Short Course, 41, 19–63.

Valley J.W., Eiler J.M., Graham C.M., Gibson E.K., Romanek C.S. and Stolper E.M. (1997)
Low-temperature carbonate concretions in the Martian meteorite ALH84001: Evidence from stable isotopes and mineralogy. Science, 275, 1633–1638.

Veizer J., Hoefs J., Lowe D.R. and Thurston P.C. (1989)
Geochemistry of Precambrian carbonates: II. Archean greenstone belts and Archean sea water. Geochimica et Cosmochimica Acta, 53, 859–871.

Veizer J., Clayton R.N., Hinton R.W., von Brunn V., Mason T.R., Buck S.G. and Hoefs J. (1990)
Geochemistry of Precambrian carbonate: 3-shelf seas and non-marine environments of the Archean. Geochimica et Cosmochimca Acta, 54, 2717–2729.

references

Veizer J., Bruckschen P., Pawellek F., Diener A., Podlaha O.G., Carden G.A.F., Jasper T., Korte C., Strauss H., Azmy K. and Ala D. (1997)
Oxygen isotope evolution of Phanerozoic seawater. **Palaeogeography, Palaeoclimatology, Palaeoecology, 132**, 159–172.

Verkouteren R.M. and Klinedinst D.B. (2004)
Value assignment and uncertainty estimation of selected light stable isotope reference materials: RMs 8543-8545, RMs 8562-8564, and RM 8566. **NIST Special Publication** 260–149, 59pp.

Vetter L., Kozdon R., Mora C.I., Eggins S.M., Valley J.W., Hönisch B. and Spero H.J. (2013)
Micron-scale intrashell oxygen isotope variation in cultured planktic foraminifers. **Geochimica et Cosmochimica Acta, 107**, 267–278.

VIM (2008)
International vocabulary of metrology – Basin and general concepts and associated terms (VIM). **Joint Committee for Guides in Metrology, Bureau International des Poids et Mesures (Sévres, France), 200:2008,** 90pp.

Warren J. (2000)
Dolomite: Occurrence, evolution and economically important associations. **Earth-Science Reviews, 52**, 1–81.

Zenger D.H., Dunham J.B. and Ethington R.L. (1980)
Concepts and models of dolomitization. Society of Economic Paleontologists and Mineralogists. **Special Publication, 28**, 320pp.

Supporting information

The following supporting information may be found in the online version of this article:

Appendix S1. Supplementary EPMA data table.

Appendix S2. Complete SIMS data table (10 μm spot size sessions).

Appendix S3. Complete SIMS data table (3 μm spot size sessions).

Appendix S4. A guide to understanding which in-text equation corresponds to each of the various calculated parameters in Appendices S2 and S3.

Appendix S5. Error propagation in the calculation of SIMS bias*(RM-UW6220)

Appendix S6. Correcting a sample measurement for SIMS $\delta^{18}O$ bias and the associated propagation of errors.

Appendix S7. Plots relating SIMS bias*(RM-UW6220) to changing Fe content along the dolomite–ankerite solid solution.

Appendix S8. Reproducibility of the assessment process of potential reference materials.

This material is available as part of the online article from: http://onlinelibrary.wiley.com/doi/10.1111/j.1751-908X.2015.00364.x/abstract (This link will take you to the article abstract).

Appendix A

Results of conventional phosphoric acid digestion and gas-source mass spectrometric analyses on the suite of UW dolomite–ankerite reference materials

WiscSIMS RM i.d.	Analysis i.d.	$\delta^{18}O$ (‰) Raw[a]	Acid-frac. factor (α)[b]	Temp. (°C)[c]	$\delta^{18}O$ (‰) (VSMOW)
UW6250	C4-246-10	30.82	1.00917	100	21.46
	C4-246-11	30.75	1.00917	100	21.39
	C4-246-14	30.71	1.00917	100	21.35
					Avg. & (2*s*) 21.40 ± (0.11)
UW6220	C4-245-4	31.95	1.00916	100	22.59
	C4-245-5	31.96	1.00916	100	22.60
	C4-245-6	31.96	1.00916	100	22.60
	C4-246-9	31.98	1.00916	100	22.61
	C4-246-13	31.96	1.00916	100	22.59
					Avg. & (2*s*) 22.60 ± (0.02)

Appendix A (continued).
Results of conventional phosphoric acid digestion and gas-source mass spectrometric analyses on the suite of UW dolomite–ankerite reference materials

WiscSIMS RM i.d.	Analysis i.d.	$\delta^{18}O$ (‰) Raw[a]	Acid-frac. factor (α)[b]	Temp. (°C)[c]	$\delta^{18}O$ (‰) (VSMOW)
UWAnk10	C4-245-21	28.91	1.00914	100	19.59
	C4-245-22	28.85	1.00914	100	19.53
	C4-245-23	28.86	1.00914	100	19.54
					Avg. & (2*s*) 19.55 ± (0.06)
UWAnk11	C4-245-17	19.72	1.00915	100	10.48
	C4-245-18	19.72	1.00915	100	10.48
	C4-245-20	19.75	1.00915	100	10.51
					Avg. & (2*s*) 10.49 ± (0.03)
UWAnk7	C4-245-2	20.55	1.00911	100	11.34
	C4-245-1	20.66	1.00911	100	11.45
	C4-245-19	20.57	1.00911	100	11.36
					Avg. & (2*s*) 11.38 ± (0.12)
UWAnk8	C4-245-14	18.41	1.00910	100	9.22
	C4-246-1	18.38	1.00910	100	9.19
	C4-246-2	18.35	1.00910	100	9.16
					Avg. & (2*s*) 9.19 ± (0.06)
UWAnk4	C4-327-2	18.39	1.00911	100	9.20
	C4-237-3	18.42	1.00911	100	9.23
	C4-327-4	18.42	1.00911	100	9.23
					Avg. & (2*s*) 9.22 ± (0.03)
UWAnk9	C4-245-9	20.86	1.00908	100	11.68
	C4-245-10	20.87	1.00908	100	11.69
	C4-245-11	20.86	1.00908	100	11.68
					Avg. & (2*s*) 11.68 ± (0.01)
UWAnk1	C4-234-2	25.03	1.00902	100	15.87
	C4-234-9	25.01	1.00902	100	15.85
	C4-234-10	25.04	1.00902	100	15.88
					Avg. & (2*s*) 15.87 ± (0.03)
UWAnk2	C4-234-6	25.06	1.00902	100	15.90
	C4-234-7	25.05	1.00902	100	15.89
	C4-234-11	25.06	1.00902	100	15.90
					Avg. & (2*s*) 15.90 ± (0.01)
UWAnk3	C4-327-6	24.98	1.00901	100	15.82
	C4-237-7	25.01	1.00901	100	15.85
	C4-327-8	24.95	1.00901	100	15.79
					Avg. & (2*s*) 15.82 ± (0.06)
	Calculated with renormalised Ca-Mg-Fe; Mn excluded				
UWAnk5cl	C4-240-9	26.21	1.00896	100	17.10
	C4-240-10	26.24	1.00896	100	17.13
	C4-240-11	26.22	1.00896	100	17.11
					Avg. & (2*s*) 17.11 ± (0.03)
	Calculated as (Ca+Mn)-Mg-Fe				
UWAnk5cl	C4-240-9	26.21	1.00896	100	17.10
	C4-240-10	26.24	1.00896	100	17.13
	C4-240-11	26.22	1.00896	100	17.11
					Avg. & (2*s*) 17.11 ± (0.03)
UWAnk6a	C4-240-5	25.09	1.00895	100	
	C4-240-7	25.14	1.00895	100	16.04
	C4-246-3	25.01	1.00895	100	15.92
					Avg. & (2*s*) 15.99 ± (0.13)

The bold values denote calculated averages and 2 standard deviations.

[a] Value measured by gas-source mass spectrometry; raw value prior to correction for phosphoric acid fractionation during carbonate digestion.

[b] Phosphoric acid fractionation factor (at 100 °C) calculated using equation 4 of Rosenbaum and Sheppard (1986) and the cation composition (Ca-Mg-Fe normalised) of each reference material (see Table 1).

[c] Carbonate phosphoric acid digestion temperature (> 4 hr).